

UNCLASSIFIED

Defense Technical Information Center  
Compilation Part Notice

ADP011213

TITLE: Optical Imaging of Objects in Turbid Medium With Ultrashort Pulses

DISTRIBUTION: Approved for public release, distribution unlimited

This paper is part of the following report:

TITLE: Optical Sensing, Imaging and Manipulation for Biological and Biomedical Applications Held in Taipei, Taiwan on 26-27 July 2000. Proceedings

To order the complete compilation report, use: ADA398019

The component part is provided here to allow users access to individually authored sections of proceedings, annals, symposia, etc. However, the component should be considered within the context of the overall compilation report and not as a stand-alone technical report.

The following component part numbers comprise the compilation report:  
ADP011212 thru ADP011255

UNCLASSIFIED

# Optical imaging of objects in turbid medium with ultrashort pulses

Chih-Yu Wang<sup>a,b</sup>, Chia-Wei Sun<sup>b</sup>,

C. C. Yang<sup>a,b,c</sup>, Yean-Woei Kiang<sup>c</sup>, Chii-Wann Lin<sup>d</sup>

<sup>a</sup>Department of Biomedical Engineering, I-Shou University, Kaoushung, Taiwan, R.O.C.

<sup>b</sup>Graduate Institute of Electro-Optical Engineering, National Taiwan University, Taipei, Taiwan, R.O.C.

<sup>c</sup>Department of Electric Engineering, National Taiwan University Taipei, Taiwan, R.O.C.

<sup>d</sup>Graduate Institute of Biomedical Engineering, National Taiwan University Taipei, Taiwan, R.O.C.

## ABSTRACT

Photons are seriously scattered when entering turbid medium; thus the images of objects hidden in turbid medium can not be obtained by just collecting the transmitted photons. Early-arriving photons, which are also called ballistic or snake photons, are much less scattered when passing through turbid medium, and contains more image information than the late-arriving ones. Therefore, objects embedded in turbid medium can be imaged by gathering the ballistic and snake photons. In the present research, we try to recover images of objects in turbid medium by simultaneously “time-gate” and “polarization-gate” to obtain the snake photons. An Argon-pumped Ti-Sapphire laser with 100fs pulses was employed as light source. A streak camera with 2ps temporal resolution was used to extract the ballistic and snake photons. Two pieces of lean swine meat, measured 4mm×3mm and 5mm×4mm, respectively, were placed in a 10cm×10cm×3cm acrylic tank, which was full of diluted milk. A pair of a polarizer and an analyzer was used to extract the light that keeps polarization unchanged. The combination of time gating and polarization gating resulted in good images of objects hidden in turbid medium.

## 1. INTRODUCTION

### 1.1 Recent development of near-infrared light imaging

Recently, optical imaging through highly scattering medium with near-infrared light has received much attention [1-8]. Because of its noninvasive nature, researchers have regarded near-infrared light as a safe alternative to ionizing radiation such as x-ray or positron emission tomography. However, near-infrared light can penetrate into biological tissues only a limited depth because of strong scatter. Therefore, advanced optical techniques are required for such imaging application.

It was shown that near-infrared light is only weakly absorbed by most biological tissues, and light propagating in biological tissues is mainly attenuated through scattering [9-11]. Based on this fact, two approaches were commonly adopted for

---

\* Correspondence: Email: [ccy@cc.ee.ntu.edu.tw](mailto:ccy@cc.ee.ntu.edu.tw); Telephone: 886-2-23657624; Fax: 886-2-23652637

imaging with near-infrared light: 1) capturing snake photons for direct imaging [2,8,12,13], and 2) collecting diffusive photons and reconstructing the image with the theory of diffuse photon density wave [1,5,10,11]. The second approach costs less than that of the first one; however, its spatial resolution is usually unsatisfied. Due to multiple scattering, the image information of the embedded objects for the diffusive light are almost lost. In fact, the spatial resolution of reconstructed images by using diffusive photons is limited by many factors, including optical properties of the turbid medium, the thickness of the samples, the wavelength of the probe light, etc. Therefore, the reconstruction of high-resolution images is not a cakewalk [14]. On the other hand, the collection of ballistic or snake photons can provide high-resolution image, but the amount of these photons are very small and not easily captured. Furthermore, these photons exist in a very short time period (200ps~300ps), dependent on the optical property of the measured tissues. In recent years, due to the development of high speed detector, such as electronic gated CCD and streak camera, the research on imaging techniques with ultrashort pulses has gradually become popular [13,15].

### **1.2 polarization gating and time gating for snake photons**

Since snake photons encounter little scattering and are along shorter path when transmitting the measured sample, they arrive at the detector earlier than diffuse photons. By gating those early arriving photons, we are able to obtain the images of the embedded objects. However, usually it is not easy to determine the time interval of snake photons. Another property of the snake photons is that their polarization almost keeps unchanged during propagation. In other words, if the incident pulse is polarized, the output snake photons bear the same polarization [16]. Therefore, combining time gating and polarization gating is useful for extracting snake-photons and get clear images.

## **2. EXPERIMENTAL PROCEDURES**

### **2.1 Samples—turbid medium and targets**

In the experiment, diluted milk (the milk was made up by milk power branded “Kolin”), was used to simulate turbid medium. The milk was contained in an transparent acrylic tank, with 10cm×10cm×3cm in dimensions. Two pieces of lean swine meat, measured 4 mm×3 mm and 5 mm×4 mm, respectively, hanged in the center of the tank and separated by about 3 mm, were embedded in the milk as objects to be imaged. The thickness of the both meat was about 1 mm. The total attenuation coefficient ( $\mu_t$ ) of the objects and the background medium are  $13.6\text{cm}^{-1}$  and  $10\text{cm}^{-1}$ , respectively. The tank was then placed on a motor-controlled two-dimensional translation stage for measurement.

### **2.2 Measurement instruments**

The experimental setup is shown in Fig. 1. An Argon-pumped Ti-Sapphire laser (Spectra Physics, USA), which emits 100fs short pulses, was employed as the light source. The streak camera was operated in the synchronous scan mode, which would accumulate the light intensity of many pulses, to obtain a high signal to noise ratio. One of the split light from the first beam splitter ( $\text{BS}_1$ ) was incident on a PIN diode to generate a trigger signal. The other part of light was separated into two paths by the second beam splitter ( $\text{BS}_2$ ). One is then incident on the samples for imaging, while the other was sent to the streak

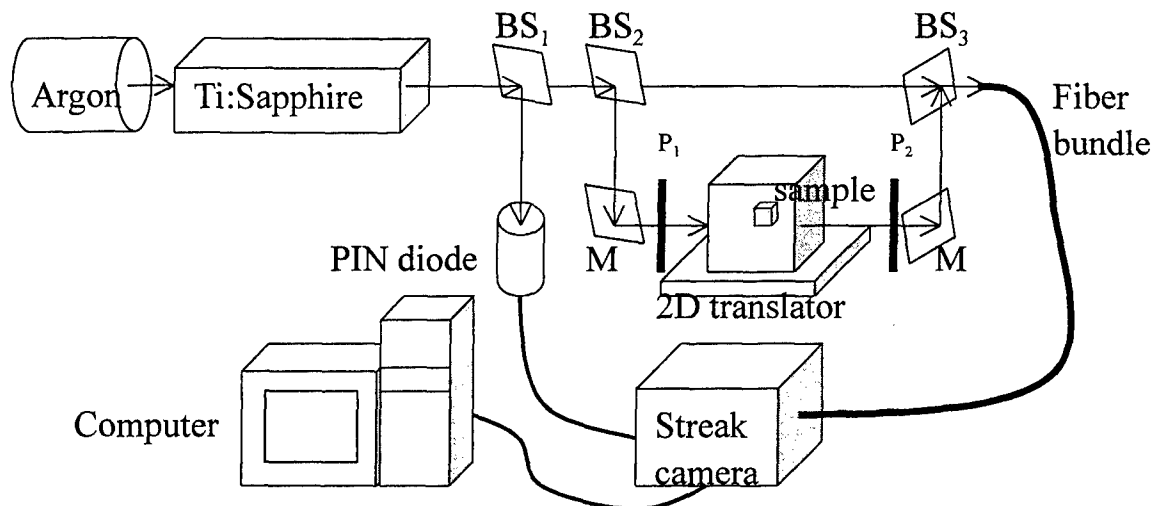


**Fig.1** Experimental setup.

camera (Hamamatsu, K.K., Japan) directly as the reference signal. During measurement, the incident light and the detector were fixed and aligned with each other, while the tank was moved with a two-dimensional motor-controlled translation stage. The measurement area was 2cm×2cm in dimensions. The temporal profiles of pulses, which were broadened (diffused) to become about 1.1 ns in width after transmitting the turbid medium, were collected point by point. Two polarizers P<sub>1</sub> and P<sub>2</sub>, placed before and after sample, were used to gating the output photons whose polarization remained unchanged. This will help the streak camera extracting the early-arriving photons, whose polarization was supposed to be unchanged.

### 2.3 Instrument control and data acquisition

The instrument control and data acquisition were implemented by using software named LabVIEW (National Instruments Inc., USA). The movement of the two-dimensional translation stage, including the moving speed, step, displacement, axis, etc, can be controlled by the self-developed software. The timing for sample moving was pre-determined to match time required for getting profiles by the streak camera. The acquired temporal profile was stored and translated into a text-format file. The data processing, including intensity normalization, temporal calibration, etc, was completed with an analysis program written in LabVIEW. After calculation, the data were stored in the hard disk, and the image was displayed on the screen.

### 3. IMAGING RESULTS

#### 3.1 Temporal profile

Temporal profiles of output pulses can be obtained by integrating the streak image for each measuring point of the sample. The reference beam, which did not pass through the turbid medium and always arrived at the detector periodically with fixed intensity, was used for time and intensity calibration. Figure 2 shows a typical temporal profile. Occasionally jitters occur due to the instability of the pulse repetition rate and laser intensity. To remove such undesired effects we normalize the intensity of the signals based on that of the reference. Also, the temporal positions of the profile were adjusted according to the center of reference. Figure 3 shows a typical calibrated temporal profile. In this chart, all data points were shifted such that the peak of the reference signal was positioned at zero time ( $t = 0$ ).

#### 3.2 Measurement with polarizers

To further reject the diffusive photons for improving the imaging results, two polarizers were placed before and behind the sample (see Fig. 1). The first polarizer ( $P_1$ ), which was placed before the sample, was used to generate a linearly polarized incident light. The second one ( $P_2$ ), which was placed behind the sample, was used as a polarization analyzer. During the measurement, the analyzer ( $P_2$ ) was first rotated to have the same orientation of  $P_1$ , and the measured signal was denoted as  $L_p$  (parallel polarization). Next, it was rotated to become perpendicular to  $P_1$ , and the measured signal was denoted as  $L_c$  (cross polarization). It is supposed that ballistic and snake photons, which are almost not scattered while propagating in the turbid medium, maintain the original polarization. However, the diffusive photons, which has been seriously scattered, have lost the original polarization information after transmitting through the scattering medium, and the orientations of polarization for such photons were random. About 50% of the diffusive light passes the parallel- and cross-polarization analyzer, respectively. Hence, the summation of  $L_p$  and  $L_c$  represents the total output light. Only those photons keeping their original polarization left in the profile of  $L_p-L_c$ . Figure 4 shows the results for summation and subtraction of  $L_p$  and  $L_c$ . In this figure, we saw that the diffusive light (the late-arriving photons) still exists in  $L_p+L_c$ , while only the ballistic and snake photons (close to the leading edge of the curve) left in the curve  $L_p-L_c$ . Therefore, we conclude that with two polarizers and a streak camera, we can extract the light keeping the original polarization, which bears abundant information for imaging.

To evaluate the possibility for optical imaging with the described method, we scanned a  $2\text{cm} \times 2\text{cm}$  area for images. The depth of the tank was about 3cm. For each measuring point, the parallel polarized light ( $L_p$ ) and cross polarized light ( $L_c$ ) were both measured. Figure 5 shows the image that was obtained from  $L_p+L_c$ , the total light passing the turbid medium. Since the signal contains diffusive photons, we can hardly recognize the shape of the targets.

On the other hand, Fig. 6 shows the image of obtained from the profile  $L_p-L_c$ . As the inset shows, only the early arriving photons (near the leading edge of the profile) are used. Further calculation shows that the contrast (defined as the image minus background to the background ratio) of the image in Fig. 6 are about 2.5 times of that in Fig. 5. In other words, in Fig. 6 the embedded objects can be identified more clearly than in Fig. 5. The white square boxes indicate the actual positions of the two pieces of meat.

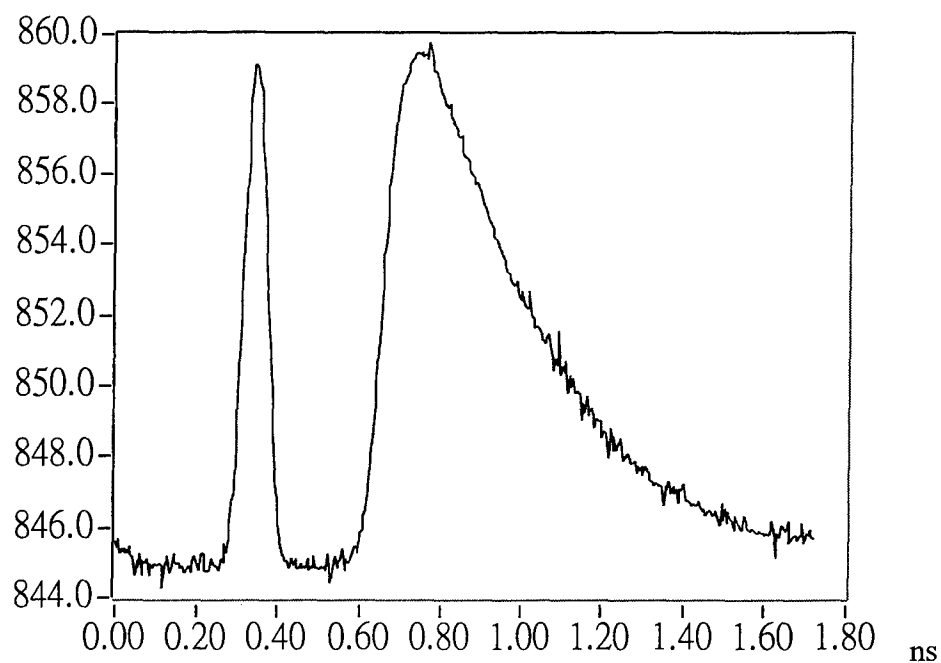


**Fig. 2** Original temporal profile obtained from the streak camera at a measuring point. The first peak represents the reference beam.

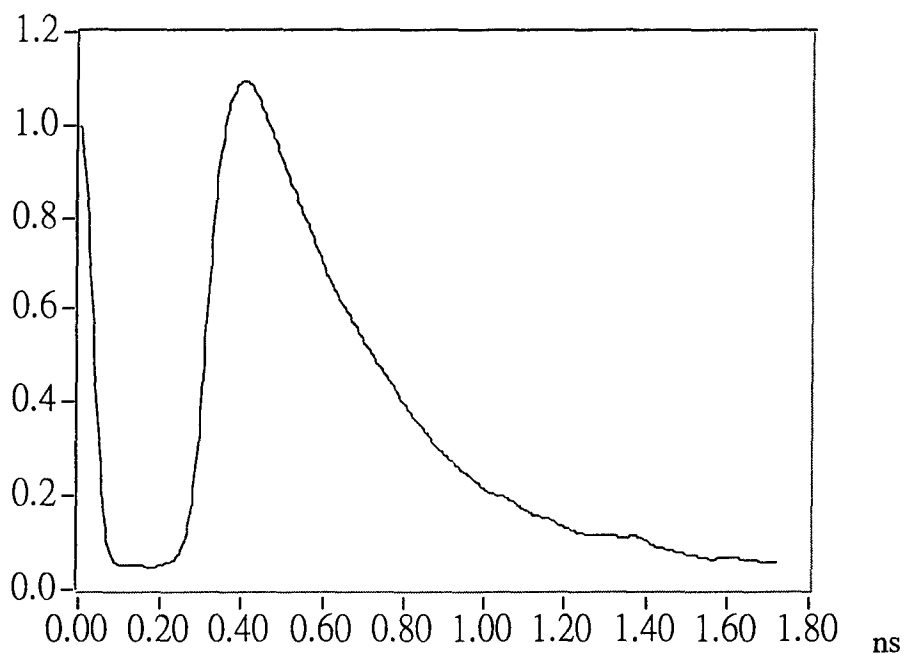


**Fig.3** Temporal-position-adjusted and intensity-normalized profile. This temporal profile has been made smooth by using a low pass filter.

#### 4. DISCUSSION AND CONCLUSION

In Fig. 6, the left image is much clearer than the right one. In fact, the right one contains more fat than the left one. Since the color of fat is almost white at room temperature, the scattering effect of this piece of meat was much severe than regular lean meat. Therefore, the image of the right one became blurrier than the left one.

In this research, by combining time gating and polarization gating, we obtained the images of biological tissues embedded in turbid medium (diluted milk). It was shown that polarization gating was an efficient approach that could help extracting ballistic and snake photons. Therefore, clearer image can be obtained. Furthermore, the addition of polarization gating provides a useful criterion for judging the interval of "snake photons", which would be very useful for the study of optical properties of tissues to be measured.

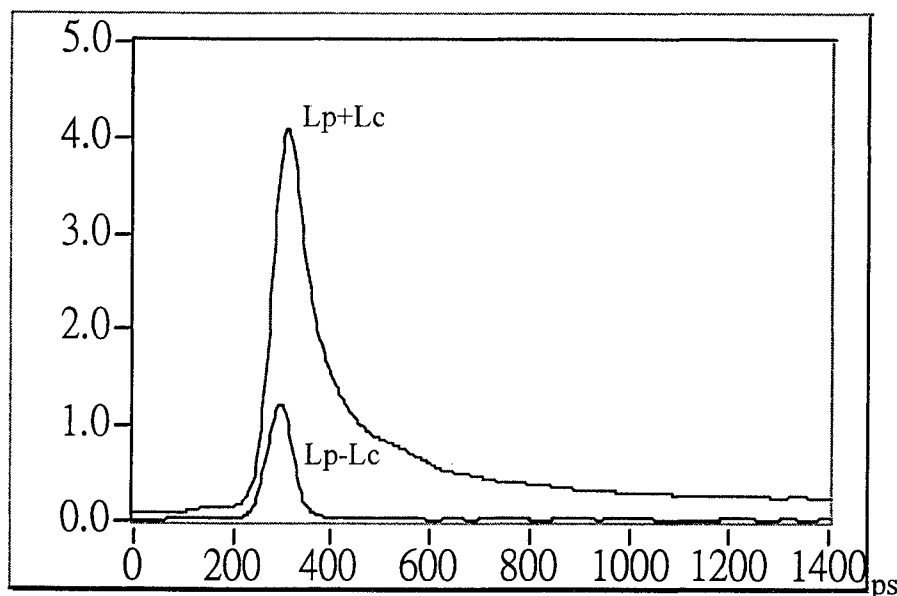


**Fig. 4** Temporal profiles for the summation of parallel- and cross-polarization light ( $L_p+L_c$ , which represents the photons passing through the sample and analyzer without considering the polarization), and the subtraction of parallel- and cross-polarization light ( $L_p-L_c$ , which represents the photons without changing their polarization after passing through the sample).

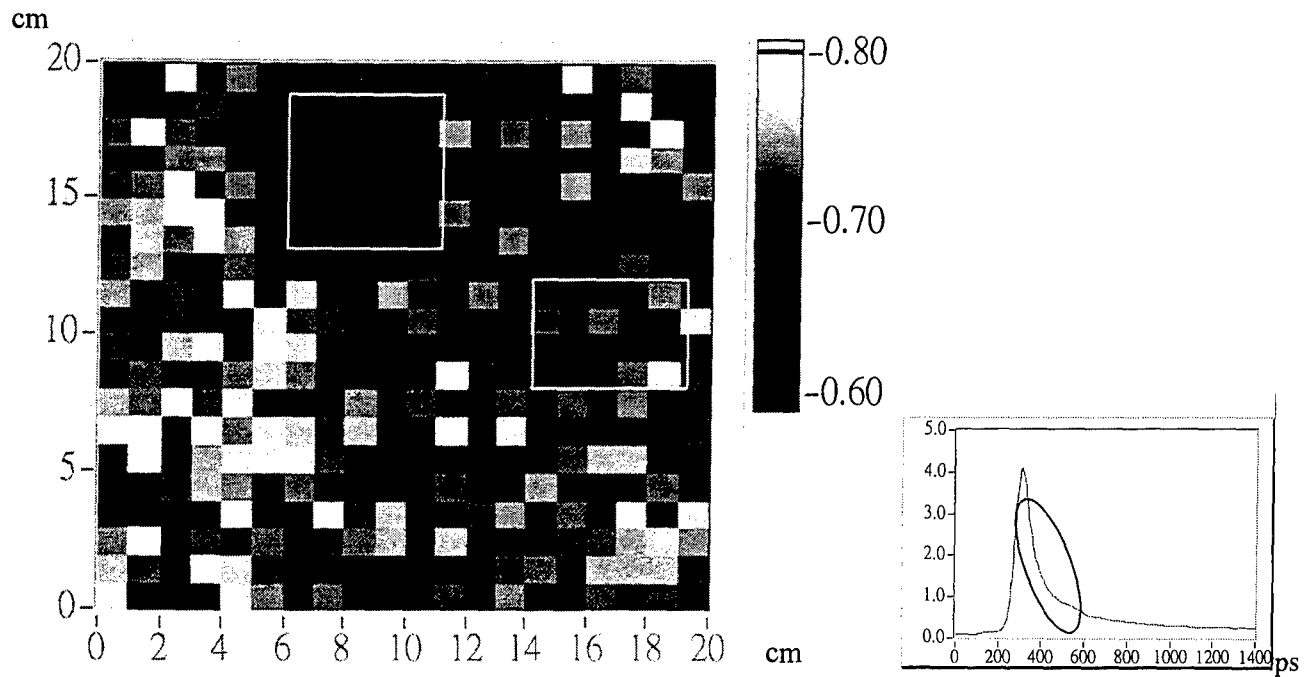


**Fig. 5** Image of objects with diffusive photons. The inset shows the resulted profile of  $L_p+L_c$ , and the interval used for calculation.

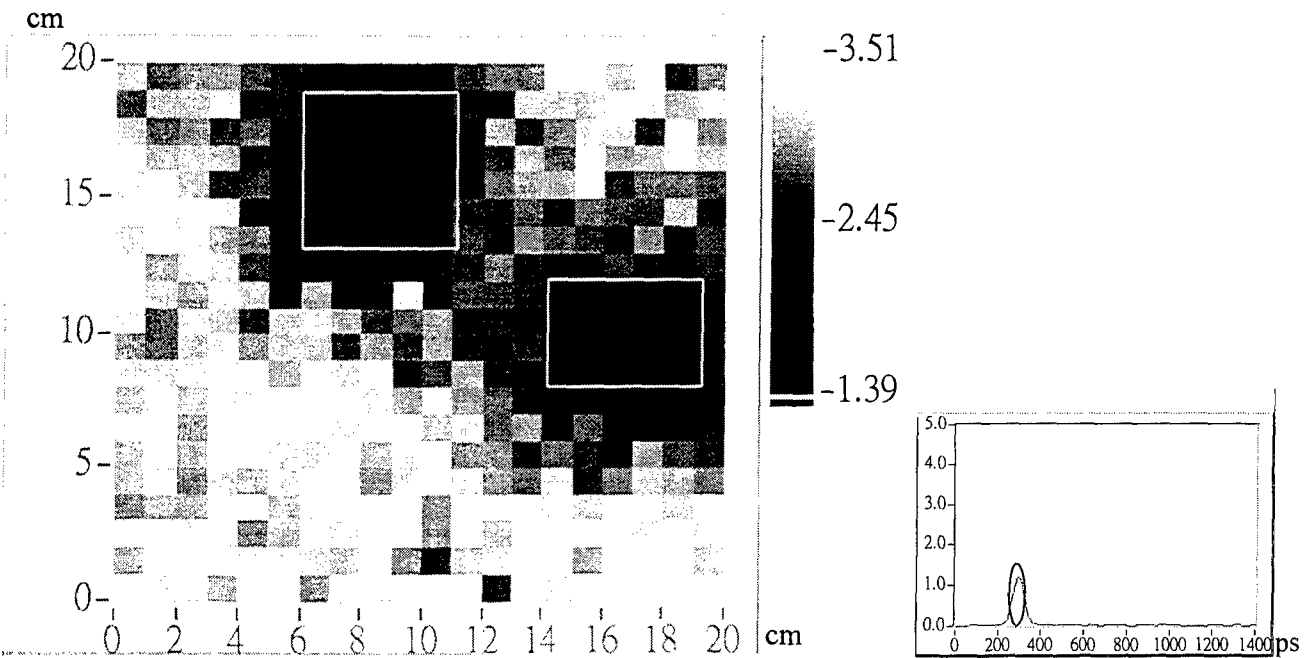


**Fig. 6** Image of objects with snake photons, which was extracted form from diffusive light with their polarization nature. The inset shows the resulted profile of  $L_p-L_c$ , and the interval used for calculation.



## REFERENCES

1. A. Ishimaru, "Diffusion of light in turbid material," *Appl. Opt.* **28**, 2210-2215, 1989.
2. L. Wang, P.P. Ho, C. Liu, G. Zhang, and R.R. Alfano, "Ballistic 2-D imaging through scattering walls using an ultrafast optical Kerr gate," *Science*. **253**, 769-771, 1991.
3. B.C. Wilson, E.M. Sevick, M.S. Patterson, and B. Chance, "Time-dependent optical spectroscopy and imaging for biomedical applications," *Proc. IEEE*. **80**, 918-930, 1992.
4. H. Jiang, K.D. Paulsen, U.L. Osterberg, B.W. Pogue, and M.S. Patterson, "Simultaneous reconstruction of absorption and scattering profiles in turbid media from near-infrared frequency-domain data," *Opt. Lett.* **20**, 2128-2130, 1995.
5. H. Jiang, K.D. Paulsen, and U.L. Osterberg, "Optical image reconstruction using DC data: simulations and experiments," *Phys. Med. Biol.* **41**, 1483-1498, 1996.
6. H. Hajime, K. Eiji, and Y. Takeaki, "Simultaneous measurements of three-dimensional reflectivity distribution in scattering medium based in optical frequency-domain reflectometry," *Opt. Lett.* **23(18)**, 1420-1422, 1998.
7. C. K. Hitzenberger and A.F. Fercher, "Differential phase contrast in optical coherence tomography," *Opt. Lett.* **24(9)**, 622-624, 1999.
8. J.C. Hebden, F.E.W. Schmidt, M.E. Fry, M. Schweiger, E. M.C. Hillman, and D.T. Depledge, "Simultaneous reconstruction of absorption and scattering images by multichannel measurement of purely temporal data," *Opt. Lett.* **24(8)** 534-536, 1999.
9. R.R. Anderson and J.A. Parrish, "The optics of skin," *J. Invest. Dermatol.* **77**, 13-19, 1981.
10. S.A. Walker, S. Fantini, and E. Gratton, "Image reconstruction by backprojection from frequency-domain optical measurements in highly scattering media," *Appl. Opt.* **36(1)**, 170-179, 1997.
11. X.D. Li, T. Durduran, A.G. Yodanis, B. Chance, and D.N. Pattanayak, "Diffraction tomography for biochemical imaging with diffuse-photon density waves," *Opt. Lett.* **22(8)**, 573-575, 1997.
12. J.C. Heden, and S.R. Arridge, "Time-resolved imaging of solid tissue phantoms using a perturbation model," *OSA TOPS on Advances in Optical Imaging and Photon Migration*. (Edited by R.R. Alfano and J.G. Fujimoto), **2**, 353-356. Optical Society of America, Washington DC, USA, 1996.
13. M.E. Zevallos, S.K. Gayen, B.B. Das, M. Alrubaiee, and R.R. Alfano, "Picosecond electronic time-gated imaging of bones in tissues," *IEEE J. Sel. Top. Quantum. Electron.* **5(4)**, 916-922, 1999.
14. J.A. Moon, R. Mahon, M.D. Duncan, and J. Reintjes, "Resolution limits for imaging through turbid media with diffuse light," *Opt. Lett.* **18(19)**, 1591-1593, 1993.
15. D. Grosenick, H. Wabnitz, H.H. Rinneberg, K.T. Moesta, and P.M. Schlag, "Development of a time-domain optical mammography and first in vivo application," *Appl. Opt.* **38(13)**, 2927-2943, 1999.
16. V. Sankaran, K. Schonenerger, J.T. Walsh Jr., and D.J. Maitland, "Polarization discrimination of coherently propagated light in turbid media," *Appl. Opt.* **38(19)**, 1999.

